Activity of the Vascular Targeting Agent Combretastatin A-4 Disodium Phosphate in a Xenograft Model of AIDS-Associated Kaposi's Sarcoma

Amyn M. Rojiani, Lingyun Li, Leroy Rise and Dietmar W. Siemann

From the Department of Interdisciplinary Oncology and Department of Pathology, H. Lee Moffitt Cancer Center and Research Institute, University of South Florida, Tampa, FL (A.M. Rojiani, L. Rise) and the Department of Pharmacology and Experimental Therapeutics (L. Li, D.W. Siemann) and Department of Radiation Oncology (D.W. Siemann), Shands Cancer Center, University of Florida, Gainesville, FL, USA

Correspondence to: Dietmar W. Siemann, PhD, Department of Radiation Oncology, University of Florida, 2000 SW Archer Road, Box 100385, Gainesville, FL 32610, USA. Tel: $+1$ 352 265 0287. Fax: $+1$ 352 265 0759. E-mail: siemadw@ufl.edu

Combretastatin A4 disodium phosphate (CA4DP) was evaluated in a xenograft model of AIDS-KS. KS xenografts were highly vascular, showing brisk mitotic activity, focal areas of necrosis, and intervening fibrovascular septae. Neoplastic cells were large or spindle-shaped, with vesicular nuclei and modest pleomorphism. Multiple junctions, microvillous-like projections, abortive lumina and rare Weibel Palade bodies were revealed by electron microscopy. Treatment with CA4DP (100 mg/kg) resulted in rapid onset of vascular effects that within 4 h resulted in an almost complete vascular shutdown in these tumors. Histological evaluation showed morphological damage within a few hours after treatment, followed by extensive necrosis which increased to $\sim 90\%$ by 24 h. At this time, viable tumor cells were evident only at the periphery of the tumor. These findings demonstrate not only the marked susceptibility of the KS model to CA4DP but also its potential application in studies related to the pathogenesis and therapy of AIDS-KS.

Kaposi's Sarcoma (KS) is a multifocal neoplasm that was previously reported to occur predominantly in older men, typically of Mediterranean origin (1). The tumor was relatively rare in the United States until the onset of the AIDS epidemic. Thereafter, a great many cases have been reported with neoplastic disease involving skin and other structures, including viscera. Despite certain differences, the classical KS and AIDS-associated tumors are considered to be different forms of the same disease. Histopathology of KS reveals highly vascularized lesions with abundant angiogenesis accompanied by abnormal blood vessel development and leakage of blood (2). The predominant cells in the tumor are the spindle-shaped cells, believed to be the tumor cells of KS. These cells express some of the surface markers of activated endothelium but also contain smooth-muscle actin, suggesting that the cell of origin may be a primitive vascular cell (3). Growth factors that support spindle-cell proliferation include interleukin (IL)-1, IL-6, and tumor necrosis factor (TNF) (1). Proteins that regulate neovascularization or angiogenesis such as

basic fibroblast growth factor (bFGF), platelet-derived growth factors, and vascular endothelial growth factor (VEGF) also promote growth of spindle cells (4).

Given the tumor's histopathology, a variety of new treatment approaches, particularly those focused on inhibiting tumor angiogenesis, are being investigated. Angiogenesis plays a crucial role in the pathogenesis and progression of KS (5) and an antiangiogenesis approach may provide a means of arresting the progression of KS. The drug that was initially tested as an angiogenesis inhibitor in patients was TNP-470. When administered once weekly by intravenous infusion, this agent gave partial responses in KS patients (6). More recently, there has been some interest in exploring the clinical utility of thalidomide as an anti-KS agent. This was based on evidence that thalidomide could inhibit angiogenesis, block tumor necrosis factor alpha (TNF-α), and inhibit intercellular adhesion molecules and basement membrane formation (7). Preliminary results from two Phase II clinical trials showed that there was activity of thalidomide in a

subset of patients with KS (8, 9). Based on the encouraging results observed with thalidomide and TNP-470, clinical research into the antiangiogenic activities of these and other agents, including interleukin-12 and angiostatin, continues (3, 7).

Another approach toward affecting the critical tumor blood supply is the application of agents that specifically damage existing tumor blood vessels (10, 11). The aim of such a vascular targeting strategy is to cause a rapid and catastrophic shutdown in the vascular function of the tumor, leading to extensive secondary tumor cell death (11, 12). Since large numbers of neoplastic cells are directly supported by small numbers of endothelial cells, damaging the tumor endothelium could have a marked impact on tumor cell survival and growth (12). Several agents that elicit irreversible vascular shutdown within solid tumors, including flavenoids (13, 14) and tubulin-binding agents (13, 15), have been identified. One class of tubulin-binding compounds, the combretastatins, inhibits microtubular activity and interferes with cell growth and proliferation (16). Of these, combretastatin A-4 disodium phosphate (CA4DP) has been shown to possess selective activity against proliferating endothelial cells (17), to inhibit endothelial cell migration (18) and to lead to rapid vascular shutdown in several preclinical tumor models (17, 19).

The goal of the present investigations was to examine and characterize the antivascular effects of CA4DP in an xenograft model of KS. While there are reports of cells derived from Kaposi's sarcoma being propagated in vitro (20–22), the tumorigenic potential of these cell lines in nude mice generally has been limited (20, 23). To carry out the current studies, the KSY-1 cell line, established from a patient with HIV-1 associated KS (24), which readily induces tumors in athymic nude mice was used.

MATERIAL AND METHODS

Cell line

In our study we used the KSY-1 cell line as characterized by Lunardi-Iskander et al. (24). This cell line was derived from mononuclear cells from pleural effusion of an AIDS patient with KS, following selective removal of lymphocytes, monocytes/macrophages and fibroblasts. The cells had originally been cultured without exogenous growth factors. In the current studies, cells were cultured in RPMI-1640 growth medium supplemented with 10% FBS, 1% Pen-Strep and 1% glutamine. KSY-1 cells were seeded (5×10^5) and passed once a week on 75-cm^2 Cell$^+$ tissue flasks that provide a positively charged surface (SARSTEDT).

Induction of tumors

KS xenografts were initiated by injecting the flanks of 6–8-week-old athymic NCR nu/nu mice (Frederick Laboratories, Frederick, MD) with 1×10^6 KSY-1 cells and were serially passed by subcutaneous transplantation of tumor pieces. Macroscopic tumors were available for experiments some 3–4 weeks later. Tumors were used at an average size of 0.5–0.7 cm diameter.

Drug treatment

CA4DP (OXiGENE Inc., Lund, Sweden) was injected intraperitoneally in a volume of 0.01 ml/g animal body weight.

Hoechst-33342 studies

Hoechst-33342 (bisBenzimide, Sigma) solution was made up in 0.9% sterile saline immediately before use. KS-bearing mice were either untreated or treated with 100 mg/kg CA4DP. Hoechst-33342 was then administered at 40 mg/kg intravenously (volume 5 ml/kg) at various times after CA4DP injection (25). One minute after Hoechst-33342 injection, the mice were killed, the tumors resected and immediately immersed in liquid nitrogen for subsequent frozen sectioning. For each tumor sample, 10 μm cryostat sections were cut at three different levels between one pole and the equatorial plane. The sections were air dried and then studied under UV illumination using a fluorescent microscope. Blood vessel outlines were identified by the surrounding halo of fluorescent H33342-labeled cells. Vessel counts were performed using a Chalkley point array for random sample analysis (26). Briefly, each section was viewed at × 10 objective magnification. A 25-point Chalkley grid was positioned randomly over the field of view. Any points falling within haloes of fluorescent cells were scored as positive. Twenty random fields were counted per section and a minimum of 6 sections per tumor was examined.

Morphologic and morphometric analyses

The tumor was dissected from the flank and adjacent connective tissue was removed. The tumor was then serially sectioned at 1 mm intervals and representative sections were submitted for routine histology after fixation in 10% neutral buffered formalin. Sections were routinely dehydrated though a series of graded alcohols, processed in xylene and embedded in paraffin. Five-μm sections derived from these paraffin blocks were routinely stained with hematoxylin and eosin (H&E), as well as Masson's trichrome stain. Tumor necrosis was assessed on stained sections using the Image Pro Plus image analysis system (Media cybernetics, Maryland). The tumor was divided into 4–8 grids using a fine permanent marker. Areas of necrosis within each grid were manually traced (as irregular areas of interest) and the percentage of necrosis determined on the Image Pro Plus system. All grid measurements were combined and the percentage of necrosis relative to the total area of the tumor was calculated.

Immunoperoxidase reactions

Tissue sections cut at 5 μm were applied to 'Plus' slides (Fisher Scientific), deparaffinized in xylene and hydrated through graded alcohols. Endogenous peroxidase was quenched using 3% H_2O_2. Antigen retrieval was enhanced for certain antibodies, by microwaving sections in citrate buffer. Following several rinses in phosphate-buffered saline (PBS, pH 7.4, 0.3% Triton X-100), the slides were incubated for 20 min in 5% normal goat serum to suppress non-specific binding of IgG. Optimal primary antibody concentration in PBS containing 0.5% BSA and 0.1% sodium azide was determined and sections were incubated for 2 h. After four PBS rinses, the slides were incubated for 15 min in a biotinylated secondary antibody (Vector Laboratories, Inc., Burlingame, CA), rinsed again and incubated in a strep-tavidin-complex reagent containing horseradish peroxidase (Zymed Laboratories, Inc., South San Francisco, CA). The slides were rinsed and incubated with the chromogen DAB (3,3′-diaminobenzidine), counterstained with hematoxylin, dehydrated through alcohols and xylene and cover-slipped with a synthetic permanent mounting medium. Antibodies used for immunoreaction of the sections are listed in the Table 1.

Electron microscopy

Sample sections of the tumor were submitted for electron microscopy in 2.5% phosphate-buffered glutaraldehyde. After fixation, the sections were osmicated in 0.1% osmium tetroxide in the above buffer, and embedded in LX-112 resin. Sections measuring 1 μm, stained with toluidine blue, were examined for presence of tumor. Ultra-thin sections were cut on a Reichert Ultracut E. The sections were placed on copper grids, double stained with uranyl acetate and lead citrate, and examined using a Phillips CM 10 electron microscope.

Table 1

Antibodies used in immunohistochemistry evaluation of Kaposi's sarcoma (KS) xenografts

| Marker	Antibody detail	Manufacturer
CD31 (PECAM-1)	Monoclonal, mouse anti-human, endothelial cell	DAKO
CD34 (QBEND10)	Monoclonal, mouse anti-human, endothelial cell	Immunotech
Factor VIIIra (vWf)	Rabbit, anti-human Factor VIII related antigen	DAKO
Muscle actin	Monoclonal, mouse anti-human myocitic cells	Ventana
Desmin	Monoclonal, mouse anti-human myocitic cells	Ventana
CD68 (KP1)	Monoclonal, mouse anti-human macrophage	DAKO

RESULTS

KSY-1 cells injected into the flanks of nude mice produced detectable tumors within 3–4 weeks. Once established, the tumors grew as solid masses, with a volume doubling time of 4–6 days. Animals were killed when the tumors reached 1.5 g in size. No metastases were noted, possibly because the observation period was short (previously it was reported that this tumor model could develop metastases after 45 days (24)). On gross examination the tumors in nude mice were vascular and appeared hyperemic.

Histologic sections of untreated KS xenografts revealed a solid, vasoformative neoplasm with intervening fibrovascular septae along with scattered inflammatory cells (Fig. 1a). The neoplastic cells were large epithelioid or spindle-shaped, with vesicular nuclei and modest pleomorphisms. The tumor was a highly vascular, actively proliferating neoplasm with brisk mitotic activity. Areas of the tumor had slit-like spaces, characteristic of endothelial-derived tumors, with scattered red blood cells, while in other areas tumor cells appear to be forming abortive lumina (Fig. 1b). Immunohistochemical analysis showed the xenografts to lack immunoreactivity for anti-factor VIII-related antigen antibody and only scattered, focal staining with CD34. CD31 immunoreactivity was seen as its characteristic membranous profile on the surfaces of blood vessels and focally within the tumor (Fig. 1c). In addition, the tumors were negative for smooth muscle markers (desmin, actin) and histiocyte marker (CD68). Electron microscopy (Fig. 1d) showed the tumor cells to be large, oval to spindle-shaped with round to irregular nuclei and prominent nucleoli. There were multiple areas where the tumor cells had microvilli that appear to be projecting into an abortive lumen. Many cells displayed tight junctions, although they differed in appearance from typical desmosomes. No virus particles were detected in the sections examined. Rod-shaped, microtubulated Weible-Palade bodies were rarely seen.

Following treatment with CA4DP (100 mg/kg), KS xenografts began to show morphological evidence of damage in tumor cells within a few hours. Twenty-four hours after CA4DP treatment, extensive necrosis could be seen with viable tumor cells detectable only at the periphery of the tumor adjacent to the surrounding normal tissues (compare Fig. 2a and b). At higher magnification, tissue destruction and nuclear fragmentation is readily evident in the entire central portion of the tumors, extending to within a few cell layers of the peripheral margin of the tumor (compare Fig. 2c and d).

To quantify the extent of necrosis produced by CA4DP treatment, sections from KS xenografts removed 24 h after treatment were assessed using an image analysis system (Fig. 3). The results showed that compared to the ∼ 10% necrosis seen in untreated tumors, treatment with 50 or 100 mg/kg CA4DP increased the extent of necrosis to ∼ 60 and ∼ 90%, respectively.
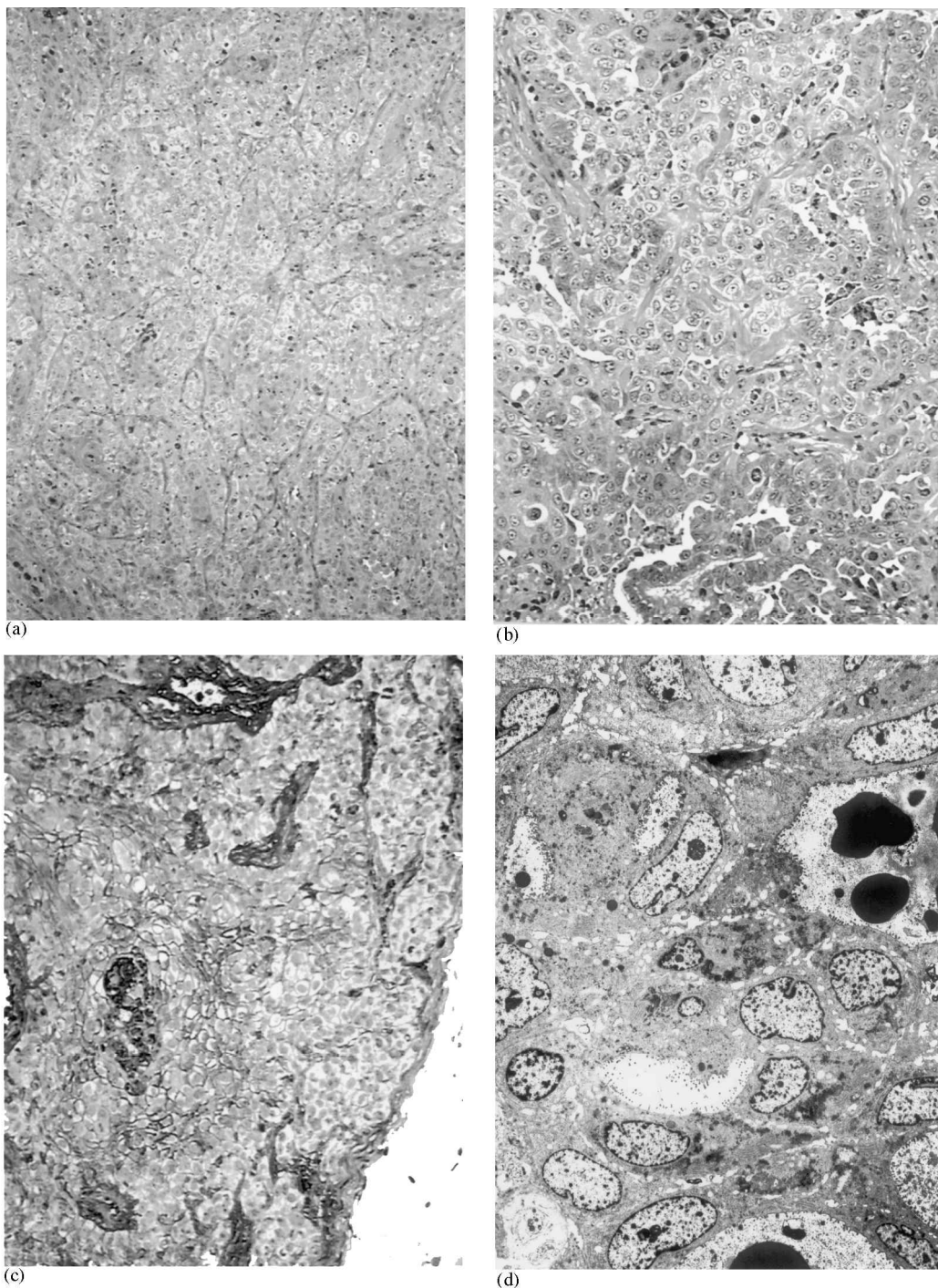
Fig. 1. (a) and (b): H&E stained, untreated Kaposi's sarcoma (KS) xenograft, original magnification ×40 (a) and ×200 (b). A solid, neoplasm with intervening fibrovascular septae can be seen in this section. Many small vessels and slit-like spaces are also visible, some containing red blood cells. The tumor cells are large, often epithelioid or spindle-shaped, and have prominent nuclei and nucleoli. (c): Untreated KS xenograft, original magnification ×20. Blood vessels and tumor cells show surface membrane immunoreaction with anti-CD31 (PECAM-1) antibody. (d): Untreated KS xenograft, electron micrograph, original magnification ×12000. Ultrastructurally, the neoplasms were large, oval to spindle-shaped with round to irregular nuclei and prominent nucleoli. Although well-defined vascular lumina containing red blood cells were present (lower left), there were multiple areas where the tumor cells had microvilli that appear to be projecting into an abortive lumen (upper right). Endothelial cells with tubuloreticulated rod-shaped bodies suggestive of Weibel-Palade bodies were rarely seen (not illustrated). Junctions were present between cells, although they differed in appearance from typical desmosomes.
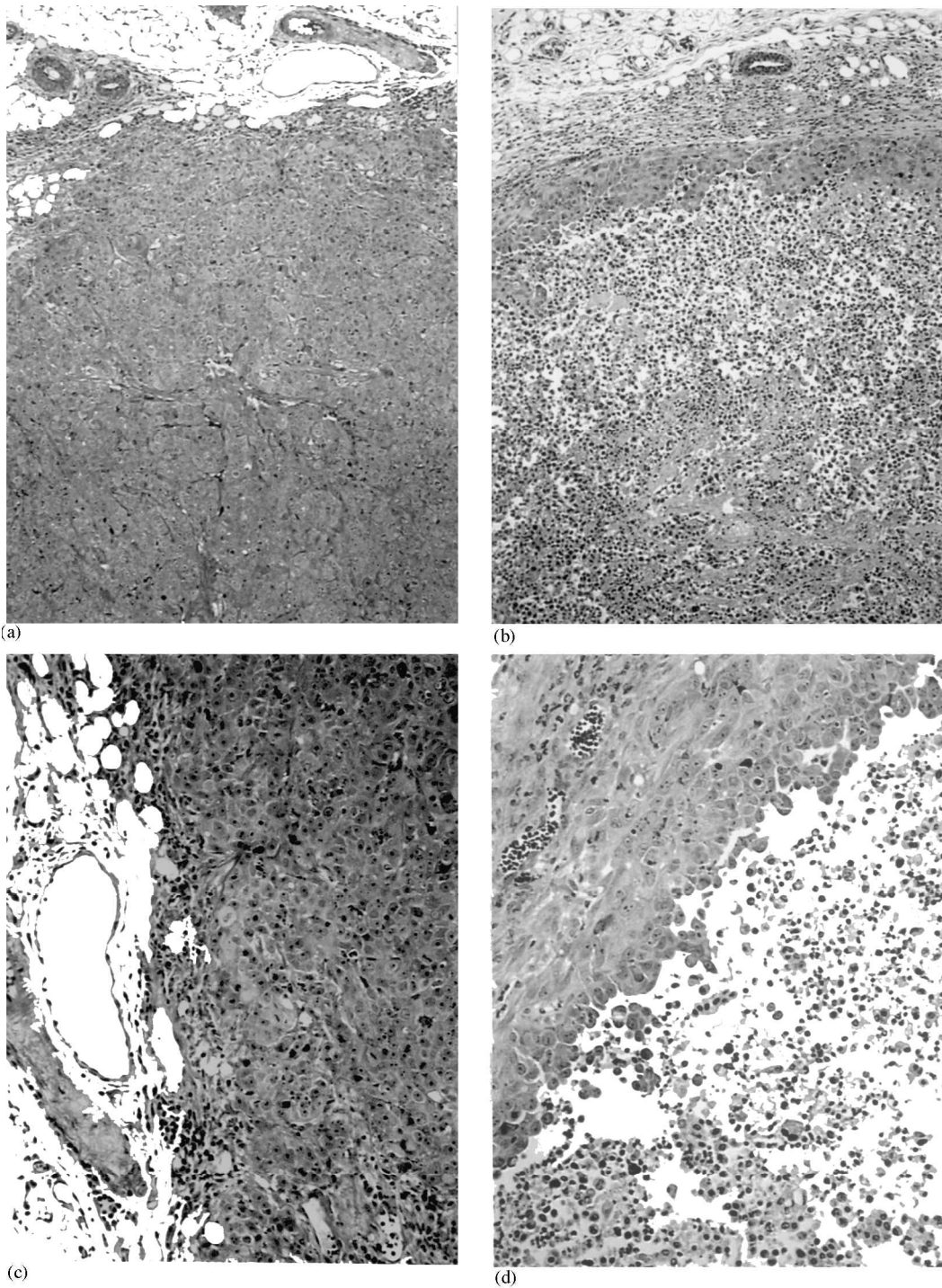
Fig. 2. (a) and (c): Untreated Kaposi's sarcoma (KS) xenograft, original magnification $\times 40$ (a) and $\times 400$ (c). Solid neoplasm with small area of surrounding normal mouse adipose, skeletal, connective tissue and blood vessels. At higher magnification (2c) the tumor also reveals scattered individual necrotic cells and details of the edge of the tumor and normal surrounding tissue. (b) and (d): CA4DP treated KS xenograft, original magnification $\times 40$ (b) and $\times 400$ (d). Following treatment with CA4DP (100 mg/kg), large areas of necrosis, involving a major portion of the tumor can be seen in this illustration. Only a small rim (3–5 cells wide) of viable tumor tissue is identifiable immediately below the normal host tissue. At higher magnification, tissue destruction and nuclear fragmentation is readily evident.
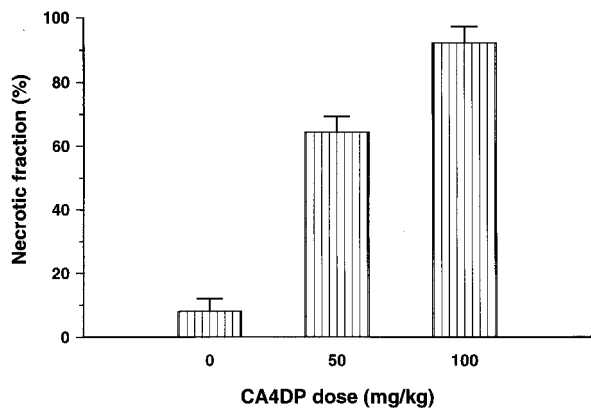
Fig. 3. The extent of necrosis in Kaposi's sarcoma (KS) xenografts assessed 24 h after the administration of a 50 or 100 mg/kg dose of CA4DP. The data are the means $\pm$ SE of 3–5 tumors.

The extensive histological changes seen in KS xenografts following CA4DP treatment were most likely the consequence of a rapid and extensive shutdown in vascular function typically associated with the in vivo action of this agent (17, 19, 27). To examine this in detail, functional vascular volume measurements based on the use of the perivascular stain Hoechst 33342 were carried out. The results showed that a single dose of 100 mg/kg CA4DP caused an almost complete vascular shutdown in KS xenografts within 4 h of treatment (Fig. 4). Compared to the abundant vasculature in control tumors, KS xenografts in mice treated with CA4DP showed functional vessels essentially only near the periphery of the tumors. This vascular
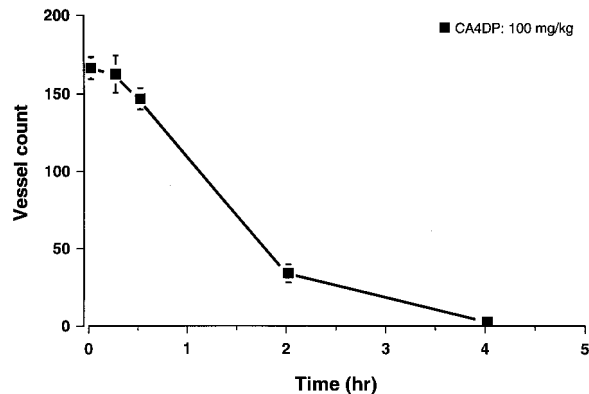

Fig. 5. Vessel counts in Kaposi's sarcoma (KS) xenografts as a function of time after treatment with a 100 mg/kg dose of CA4DP. At a given time after CA4DP treatment, mice were injected with Hoechst 33342 (40 mg/kg) to identify patent vessels, and tumors were removed 1 min later. Counting was performed using a Chalkley point array for random sample analysis. Data are the means $\pm$ SE of 5 tumors.

damaging effect of CA4DP occurred rapidly and could be detected in KS xenografts within 30 min of drug treatment. Indeed, when functional vessels were counted (Fig. 5), most were found to be shut down 2 h after CA4DP exposure.

DISCUSSION

Treatment for AIDS-KS has been relatively ineffective and despite some recent advances in the management of this
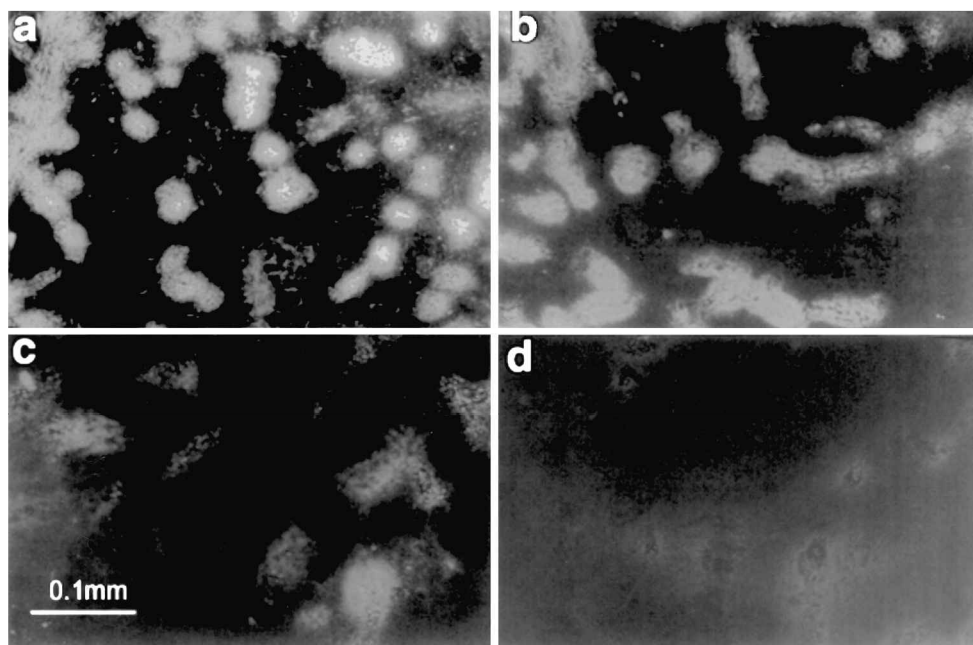

Fig. 4. Patent blood vessels, identified by the surrounding fluorescent tumor cells in Kaposi's sarcoma (KS) xenografts removed 1 min after an iv injection of 40 mg/kg Hoechst 33342. Tumors were from untreated mice (a) or from mice that had received a 100 mg/kg dose of CA4DP 30 min (b), 2 h (c) or 4 h (d) earlier. Magnification $\times$ 32.

disease, continued pursuit of more effective therapies is needed. The disorder has considerable morbidity and its lack of satisfactory responses to traditional therapeutic interventions makes it an excellent candidate for new therapeutic strategies such as a vascular targeted approach. The availability of a reliable and reproducible animal model of Kaposi's sarcoma would greatly facilitate preclinical therapeutic investigations. Although many cell lines have been cultured from individuals with HIV infection, the ability of these cells to induce tumors in nude mice has been limited. However, KSY-1 cells do not appear to suffer this shortcoming. This cell line, which was originally derived from a patient with AIDS (24), produced tumors with morphologic, immunohistochemical, and ultra-structural features (Figs. 1 and 2) that bear a strong similarity to biopsy-derived material from the tumors of AIDS patients. Similarly, although the etiology and pathogenesis of Kaposi's sarcoma remain elusive, and its cell of origin remains controversial, it is generally believed that endothelial-derived cells are the most likely candidates (3). Again, the histologic appearance of endothelial characteristics including slit-like spaces, abortive lumina, and the general endothelial nature of the cells in the KS xenografts (Figs. 1 and 2) supports the accuracy of this model.

Given the tumor's fundamental characteristics, it is logical that therapies targeting the angiogenic process should be considered for the management of this disease. Indeed clinical trials utilizing two such agents (TNP 470 and thalidomide) are currently ongoing (6, 8, 9). Recently, lead compounds based on a strategy that aims to cause direct damage to the tumor endothelium resulting in rapid and catastrophic shutdown in the vascular function of the tumor and leading to extensive secondary tumor cell death (11) also have entered clinical trials. One of these, CA4DP, has shown preferential cytotoxicity to dividing endothelial cells in vitro as well as reductions in blood flow and induction of necrosis in a variety of preclinical tumor models (17). These vascular effects of CA4DP were achieved with a large therapeutic window (17, 19, 27). Perhaps most importantly, Phase I observations have demonstrated that CA4DP doses that lead to reductions in tumor blood flow can readily be reached in patients (28).

The present investigations demonstrate that the pathophysiological effects of CA4DP observed in KS xenografts were similar to those previously reported by our laboratory in the rodent KHT sarcoma model (27). CA4DP treatment resulted in a rapid induction of vascular damage in these tumors such that within 4 h of treatment vascular shutdown was almost complete (Figs. 4 and 5). This was followed by extensive secondary tumor cell death caused by ischemia (Figs. 2 and 3). Histological assessments showed extensive hemorrhagic necrosis 24 h after CA4DP was administered systemically to KS tumor-bearing mice, with only a small rim of viable tumor cells surviving near

the periphery of the tumor (Fig. 2). These tumor cells probably survived because they were close to the surrounding normal tissues where they were supplied with nutrients from the normal tissue vasculature that was not affected by the action of CA4DP. This notion along with the high level of necrosis ($\sim 90\%$, Fig. 3) induced by a 100 mg/kg dose of CA4DP, also would argue that higher single dose CA4DP exposures would have little additional effect on KS xenografts, a conclusion borne out by subsequent analyses of clonogenic cell survival and tumor growth delay (29). Thus despite the significant antivascular effects and extensive cell death and necrosis caused by a dose of CA4DP equivalent to $< 1/10$, the maximum tolerated dose, it is clear that alternative approaches need to be considered to eliminate the tumor cells which survive because of their location near normal blood vessels. In order to maximize the utility of this antivascular agent, CA4DP treatment ought to be applied either as multiple repeat exposures administered at times when the surviving tumor tissue attempts to re-establish a tumor vessel network or in an adjuvant setting with conventional anticancer therapies such as radiotherapy or chemotherapy targeted to the surviving tumor cells (30).

In conclusion, KS xenografts initiated from KSY-1 cells display characteristics of endothelial cell origin and bear close pathologic resemblance to reported biopsy-derived Kaposi's sarcoma pathology. The model's similar biological, morphological and immunophenotype may thus prove to be a valuable adjunct for studies related to pathogenesis and therapy of AIDS-KS. In particular, in a preclinical setting, this model appears to be well suited to providing an excellent opportunity to evaluate therapeutic investigations based on antivascular or antiangiogenic principles. Furthermore, the significant response of KS xenografts to the antivascular targeting agent CA4DP suggests that serious consideration should be given to evaluation of this agent in patients with AIDS-KS in future Phase II clinical trials.

ACKNOWLEDGEMENT

REFERENCES

1. Sung JCY, Louie SG, Park SY. Kaposi's sarcoma: advances in tumor biology and pharmacotherapy. Pharmacotherapy 1997; 17: 670–83.
2. Gallo RC. The enigmas of Kaposi's sarcoma. Science 1998; 282: 1837–9.
3. Kroll MH, Shandera WX. AIDS-associated Kaposi's sarcoma. Hosp Pract 1998; 33: 99–102.
4. Nakamura S, Sakurada S, Salahuddin SZ, et al. Inhibition of development of Kaposi's sarcoma-related lesions by a bacterial cell wall complex. Science 1992; 255: 1437–40.
5. Cornali E, Zietz C, Benelli R, et al. Vascular endothelial growth factor regulates angiogenesis and vascular permeability in Kaposi's sarcoma. Am J Pathol 1996; 149: 1851–69.

6. Dezube BJ, VonRoenn JH, Holden-Wiltse J, et al. Fumagillin analog in the treatment of Kaposi's sarcoma: a phase I AIDS clinical trial group study. AIDS Clinical Trial Group No. 215 Team. J Clin Oncol 1998; 16: 1444–9.

7. Gascon P, Schwartz RA. Kaposi's sarcoma. New treatment modalities. Dermatol Clin 2000; 18: 169–75.

8. Fife K, Howard MR, Gracie F, et al. Activity of thalidomide in AIDS-related Kaposi's sarcoma and correlation with HHV8 titre. Int J STD AIDS 1998; 9: 751–5.

9. Little RF, Wyvill KM, Pluda JM, et al. Activity of thalidomide in AIDS-related Kaposi's sarcoma. J Clin Oncol 2000; 18: 2593–602.

10. Denekamp J. The current status of targeting tumour vasculature as a means of cancer therapy—an overview. Int J Radiat Biol 1991; 60: 401–8.

11. Denekamp J. Angiogenesis, neovascular proliferation and vascular pathophysiology as targets for cancer therapy. Br J Radiol 1993; 66: 181–96.

12. Bicknell R, Harris AL. Anticancer strategies involving the vasculature: vascular targeting and the inhibition of angiogenesis. Semin Cancer Biol 1992; 3: 399–407.

13. Hill SA, Sampson LE, Chaplin DJ. Anti-vascular approaches to solid tumor therapy: evaluation of vinblastine and flavone acetic acid. Int J Cancer 1995; 63: 119–23.

14. Zwi LJ, Baguley BC, Gavin JB, et al. Blood flow failure as a major determinant in the antitumor action of flavone acetic acid. J Natl Cancer Inst 1989; 81: 1005–13.

15. Baguley BC, Holdaway KH, Thomsen LL, et al. Inhibition of growth of colon 38 adenocarcinoma by vinblastine and colchicine. Evidence for a vascular mechanism. Eur J Cancer 1991; 27: 482–7.

16. Pettit GR, Singh SB, Hamel E, et al. Isolation and structure of the strong cell growth and tubulin inhibitor combretastatin A-4. Experientia 1989; 45: 209–11.

17. Dark GG, Hill SA, Prise VE, et al. Combretastatin A-4, an agent that displays potent and selective toxicity toward tumor vasculature. Cancer Res 1997; 57: 1829–34.

18. Grosios K, Holwell SE, McGown AT, et al. In vivo and in vitro evaluation of combretastatin A-4 and its sodium phosphate prodrug. Br J Cancer 1999; 81: 1318–27.

19. Horsman MR, Ehrnrooth E, Ladekarl M, et al. The effect of combretastatin A-4 disodium phosphate in a C3H mouse mammary carcinoma and a variety of murine spontaneous tumours. Int J Radiat Oncol Biol Phys 1998; 42: 895–8.

20. Wittek AE, Mitchell CD, Armstrong GR, et al. Propagation and properties of Kaposi's sarcoma-derived cell lines obtained from patients with AIDS: similarity of cultured cells to smooth muscle cells. AIDS 1991; 5: 1485–93.

21. Benelli R, Repetto L, Carlone S, et al. Establishment and characterization of two new Kaposi's sarcoma cell cultures from an AIDS and a non-AIDS patient. Res Virol 1994; 145: 251–9.

22. Bonish BK, Foreman KE, Gutierrez-Steil C, et al. Phenotype and proliferation characteristics of cultured spindle-shaped cells obtained from normal human skin and lesions of dermatofibroma, Kaposi's sarcoma, and dermatofibrosarcoma protuberans: a comparison with fibroblast and endothelial cells of the dermis. J Dermatol Sci 1997; 16: 52–8.

23. Herndier BG, Werner A, Arnstein P, et al. Characterization of a human Kaposi's sarcoma cell line that induces angiogenic tumors in animals. AIDS 1994; 8: 575–81.

24. Lunardi-Iskandar Y, Gill P, Lam VH, et al. Isolation and characterization of an immortal neoplastic cell line (KSY-1) from AIDS-associated Kaposi's sarcoma. J Natl Cancer Inst 1995; 87: 974–81.

25. Smith KA, Hill SA, Begg AC, et al. Validation of the fluorescent dye Hoechst 33342 as a vascular space marker in tumours. Br J Cancer 1988; 57: 247–53.

26. Curtis ACS. Area and volume measurements by random sampling methods. Med Biol Illustra 1960; 10: 261–6.

27. Li L, Rojiani A, Siemann DW. Targeting the tumor vasculature with combretastatin A-4 disodium phosphate: effects on radiation therapy. Int J Radiat Oncol Biol Phys 1998; 42: 899–903.

28. Randal J. Antiangiogenesis drugs target specific cancers, mechanisms. J Natl Cancer Inst 2000; 92: 520–2.

29. Li L, Rojiani AM, Siemann DW. Preclinical evaluations of therapies combining the vascular targeting agent combretastatin A-4 disodium phosphate and conventional anticancer therapies in the treatment of Kaposi's sarcoma. Acta Oncol 2002; 41: 91–7.

30. Siemann DW, Warrington KH, Horsman MR. Targeting tumor blood vessels: an adjuvant strategy for radiation therapy. Radiother Oncol 2000; 57: 5–12.